Next Energy xxx (xxxx) xxx

Contents lists available at ScienceDirect

Next Energy

journal homepage: www.sciencedirect.com/journal/next-energy

Direct recycling of carbon black and graphite from an aqueous anode slurry of lithium-ion batteries by centrifugal fractionation

Tolga Yildiz [a,*], Patrick Wiechers [a], Hermann Nirschl [a], Marco Gleiß [a]

[a] Karlsruhe Institute of Technology (KIT), Institute for Mechanical Process Engineering and Mechanics - Process Machines, Straße am Forum 8, 76131 Karlsruhe, Germany

ARTICLE INFO

Keywords:
Direct battery recycling
Decanter centrifuge
Graphite
Carbon black
Particle size analysis
Sedimentation analysis

ABSTRACT

Centrifugation is a promising method for direct recycling of lithium-ion battery materials from an aqueous slurry. The present work investigates the continuous fractionation of an aqueous anode slurry into the active material graphite and the conductive carbon black in a decanter centrifuge. To evaluate the separation success, two analytical methods utilizing the different particle sizes and sedimentation velocities of the materials were developed and tested. Both methods can detect graphite separation efficiencies up to 90 % based on centrate samples. The detectability of carbon black in sediment samples is more sensitive for the sedimentation analysis, which can measure carbon black separation efficiencies down to 1 %, in contrast to the particle size analysis, allowing the detection of separation efficiencies down to 10 %. Both methods provide similar results in terms of assessing the separation process in the lab-scale decanter centrifuge. At a centrifugal acceleration of 352 g and a volume flow of 66 l/h, more than 90 % graphite can be separated with a low carbon black deposition between 10 % and 20 %. Thus, a high recovery of graphite and carbon black from an aqueous anode slurry by using a decanter centrifuge is basically possible.

1. Introduction

The demand for functional materials of the lithium-ion battery (LIB) is increasing tremendously in the context of the progressing electromobility and the energy supply revolution. LIB plays a special role due to its high energy density and lifetime [1–4]. To fully meet the demand for LIB, recycling of the functional materials of spent batteries is essential in the future. The currently applicable directive 2006/66/EC of the European Commission [5] requires a recovery of at least 50 % of the LIB for environmentally compatible battery disposal. The focus of already established pyro- and hydrometallurgical recycling processes is especially on the recovery of the economically valuable metals such as copper, lithium, cobalt, and nickel [6–8]. A planned revision of directive 2006/66/EC strengthens the minimum recycling rates for copper, cobalt, and nickel to 95 % and for lithium to 80 % until 2031, according to the European Council report [9]. The recovery of graphite, which is widely used as anode active material, will also gain relevance in the long term [10–12]. The European Council report [9] also identifies graphite as a critical raw material, as well as lithium and cobalt, emphasizing the need for graphite recycling to ensure material supply chains for battery production.

A variety of different process routes exist for LIB recycling, using mechanical, pyrometallurgical, and hydrometallurgical processes in different combinations. Velázquez-Martínez et al. [13] provide an overview of the industrially established and emerging LIB recycling processes. It can be seen that often mechanical methods are used in the first steps. Shredders, crushers, and grinders are used to break down the battery into its component parts. Mechanical separation apparatuses such as screens, separating tables, classifiers, and magnetic separators exploit the different physical properties of the materials to sort coarse fragments such as conductor foils or housing parts and to separate them from the fine particulate black mass consisting mainly of active materials and conductive carbon black.

Pyrometallurgical and hydrometallurgical methods are especially used for the recovery of valuable metals in the black mass. Pyrometallurgical processes recycle and purify the metals by physical transformations and chemical reactions at high temperatures. Metallic elements such as cobalt and nickel are recovered as alloys, while lithium can be found in the resulting slag [14,15]. Hydrometallurgical recycling first converts solid metals into dissolved ions by acids, alkalis, or bacterial solutions in the leaching step. Then, the metals are selectively recovered by a series of precipitation, extraction, or electrolysis methods

* Corresponding author.
E-mail address: tolga.yildiz@kit.edu (T. Yildiz).

https://doi.org/10.1016/j.nxener.2023.100082
Received 14 July 2023; Received in revised form 23 October 2023; Accepted 8 November 2023

[16,17]. Pyrometallurgical recycling is simple and mature. However, the valuable graphite and other organic components are completely lost in the process, and further hydrometallurgical processes are required to recover the pure metals from the alloys and slag. Although hydrometallurgy does not require high energy consumption and exhaust gas treatment as in pyrometallurgy due to operation at low temperatures and materials are recovered with high purity, costly wastewater treatment is necessary due to the high chemical input [18,19].

An alternative approach is direct battery recycling. In contrast to hydro- and pyrometallurgy, this approach recovers and processes battery materials while preserving their original structure and function to return them directly to the LIB supply chain. For the direct recovery of the materials, processes for separating the materials that utilize the different physical properties of the materials are used first, before methods for regenerating especially the degraded active materials are applied [20–22]. Mechanical separation processes prior to pyro- and hydrometallurgy sort coarse fragments already after liberating the components and separate them from the fine particulate black mass. For purely direct battery recycling without pyro- and hydrometallurgy, one approach is to apply this separation principle to the particulate black mass as well.

Froth flotation already exists as a direct method to separate nickel-manganese-cobalt oxides (NMCs) or lithium cobalt oxides (LCOs) as cathode active materials and graphite as anode active material from the black mass according to their different physicochemical properties [23–25]. Another promising method for recovering particulate components of the black mass is centrifugation, already used in various fields of mechanical solid-liquid separation, e.g., for liquid purification, particle dewatering, or fractionation and sorting of particles [26,27]. For fractionation or sorting a heterogeneous particulate mixture, as in the case of black mass, the separation principle of centrifugation is based on the different settling behavior of particles due to centrifugal forces acting on the particle in a fluid phase. In addition to the speed, the geometry of the centrifuge, and properties of the fluid phase, particle properties, such as density, particle size, or particle shape, determine the settling behavior of the particles in the centrifugal field [28].

In the field of direct battery recycling, studies already exist that apply the separation principle to recover cathode and anode active materials from a black mass. Due to the density difference between cathode and anode active materials, one approach is to use heavy liquids with a density between the two materials, causing the heavy cathode active material to accumulate at the bottom and the lighter anode active material to accumulate at the top of the liquid phase in a centrifugal field [29,30]. Al-Shammari and Farhad [31] even showed that the method allows to separate different cathode active materials differing in their densities. However, it is important to keep in mind that heavy liquids are costly and therefore also require a recycling concept. In contrast, Zhang et al. [32] applied centrifugation without heavy liquids to separate an aqueous black mass slurry consisting of the cathode active material $LiCoO_2$ and the anode active material graphite in a Falcon centrifugal concentrator. Due to the higher density and particle size of $LiCoO_2$ compared to graphite particles, an underflow $LiCoO_2$ recovery efficiency of about 73 % was achieved in this case with an overflow graphite recovery efficiency of about 69 %. Also using a Falcon Ultra-Fine concentrator, Zhan and Pan [33] investigated the potential of centrifugation for separating the cathode active material NMC111 and the anode active material graphite from a aqueous black mass slurry. After several separation steps, a recovery of NMC111 with a higher density than graphite is achievable with a purity of at least 98 % in the concentrate stream. On the other hand, Wolf et al. [34] analyzed the approach of using centrifugation to recycle the heavy cathode active material lithium iron phosphate and the light conductive additive carbon black, which is hardly considered in previous LIB recycling processes, from an aqueous slurry. Under optimized process conditions, complete separation of lithium iron phosphate was obtained in a tubular centrifuge, while about 34 % of carbon black was recovered in the centrate.

Having demonstrated the potential of centrifugation for fractionation of an aqueous cathode slurry, the next challenge is to apply the separation mechanism to anode materials in an aqueous slurry. A suitable apparatus to fulfill this separation task is the decanter centrifuge, already widely used in numerous applications such as wastewater treatment or in the mining industry for separating, concentrating, deliquoring, classifying, and fractionating in solid-liquid separation while realizing high throughputs [35,36]. The present work analyzes the fractionation of an aqueous anode slurry into the active material graphite and the conductive additive carbon black, differing significantly in particle size and density, in a decanter centrifuge. The purpose is to verify the suitability of centrifugation in a decanter centrifuge for separating an anode slurry as a possible process of direct battery recycling, offering advantages over existing hydro- and pyrometallurgical battery recycling, as mentioned before. To achieve this purpose, it is necessary to distinguish between graphite and carbon black in an aqueous slurry. As the two materials have the same chemical composition, their detection in an aqueous slurry is challenging. Therefore, another objective of this work is the development and testing of analytical methods for the determination of graphite and carbon black concentrations in an aqueous anode slurry. This is required to monitor the process for different operation conditions and to finally evaluate the use of a decanter centrifuge for the direct recycling of anode slurries. Particle size analysis by laser diffraction and sedimentation analysis by the LUMiSizer© are available as two analytical instruments having the potential to distinguish the two particle systems in aqueous slurries based on their different physical properties. First, the developed methods are presented and their suitability for the determination of graphite and conductive carbon black contents in aqueous slurries is analyzed. Using the two tested methods, experiments were then carried out investigating the fractionation of an aqueous anode slurry into graphite and conductive carbon black in a decanter centrifuge.

2. Material and methods

2.1. Anode materials

The basis for the investigations were water-based anode slurries made from the common active material graphite, the conductive additive carbon black, and the water-processable binder materials carboxymethylcellulose (CMC) and styrene butadiene rubber (SBR). Such electrodes do not require the toxic, flammable, and expensive solvent 2-N-pyrollidone (NMP), which is used as a standard in combination with the binder material polyvinylidene (PVDF) in LIB. As a result, water-based electrodes are increasingly playing a more important role to make both the manufacturing and direct recycling of LIB more environmentally friendly and safer while providing comparable electrochemical performance to conventional PVDF-based electrodes [37,38].

Graphite MECHANO-CAP® 1P1 (HC Carbon Gmbh) with a solid density of 2200 kg/m^3 was used as anode active material. Carbon Black SUPER C65 (Nangrafi Nano Technology) with a smaller solid density of 1600 kg/m^3 in contrast to graphite acted as the conductive additive. Fig. 1 shows graphite and carbon black particles imaged with a scanning electron microscope. The investigated graphite particles have a pebble-like shape, while carbon black particles represent branched agglomerate or aggregate structures formed from nanometer-sized, spherical primary particles. In addition to the different particle shapes, the particle size differences of the two materials are already apparent here, which can be seen more clearly in the particle size analysis using laser diffraction presented in Chapter 2.3.1. The water-soluble binder material CMC is provided from Sigma-Aldrich GmbH. The SBR used (Targray International Inc.) is provided in an aqueous dispersion with a solid fraction of 15 %.

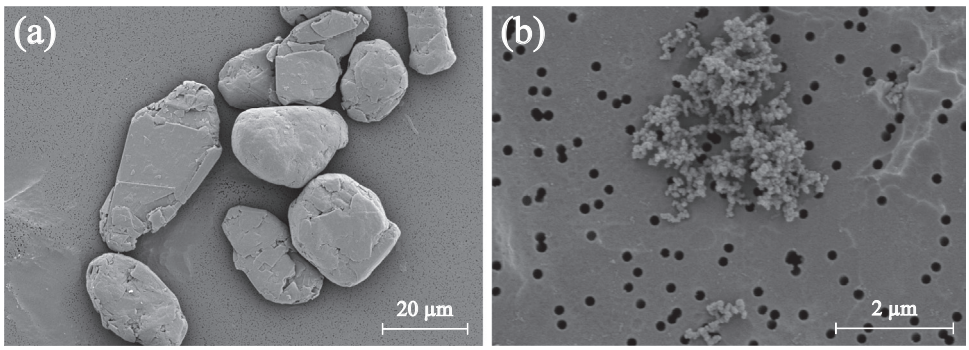

Fig. 1. Scanning electron microscope images of (a) graphite particles (magnification: 1000x, high voltage: 5 kV, work distance: 15 mm) and (b) carbon black particles (magnification: 5000x, high voltage: 2.5 kV, work distance: 16 mm).

2.2. Preparation of the aqueous anode slurries

The aqueous anode slurry used for the studies of the fractionation process in the decanter centrifuge is prepared in a vessel using a three-blade propeller stirrer. The solid mass ratio between graphite, carbon black, CMC, and SBR is 90:7:1.5:1.5 with a total solid volume fraction of 14.3 %. The solid volume fraction of graphite is 12.9 %, while the carbon black particles have a solid volume fraction of 1.4 % in the slurry. In the first step, the binder CMC is completely dissolved in deionized water for at least 12 h at a speed of 400 rpm. This is followed by the addition of carbon black with further deionized water. After the carbon particles are dispersed at a speed of about 1000 rpm for about 30 min, the graphite particles are added with the remaining deionized water. Finally, the SBR dispersion is added and the suspension is further dispersed at a lower speed of about 400 rpm. In this work, this aqueous anode slurry, which is similar to conventional anode slurries in terms of the composition of graphite, carbon black, and binders and is used for the fractionation investigated in the decanter centrifuge, is designated as the original anode slurry.

The solid volume fraction of the investigated anode slurry is lower than in conventional anode slurries. The reason is that the proof of concept for separating an anode slurry by centrifugation should first be investigated for this simpler case. The solid volume fraction determines the distance between the particles in the liquid phase and thus the settling behavior of the particles [39,40]. At low fractions, larger distances between the particles exist, causing the particles to settle at different velocities according to their physical properties, such as particle size, particle density, or particle shape. This is crucial for the centrifugal fractionation of a slurry with two particle materials differing in their physical properties and correspondingly in their individual settling velocities. When the solid volume fraction is significantly increased, the particle distances are reduced, resulting in mutual hindering of the particles during settling due to hydrodynamic and interparticle interactions. As a result, the particles settle as a collective in a sharp settling front at a much lower sedimentation velocity than at lower fractions, and their physical material properties lose their individual influence on the settling behavior. Thus, no separation of the two materials in the slurry occurs in a centrifugal field. Furthermore, a higher solid volume fraction leads to a higher fraction of the CMC binder, causing an increase in the viscosity of the liquid phase and leading to a generally slower particle settling in the centrifugal field. In this context, it is questionable if particle deposition and thus fractionation is still possible with the speed and residence time range of the decanter centrifuge at all.

For testing the available analytical methods to determine graphite and carbon black fractions in aqueous anode slurries, graphite-free (pure carbon black slurry) and carbon-black-free anode slurries (pure graphite slurry) as well as anode slurries with reduced graphite or carbon black fractions compared to the original anode slurry were additionally prepared. The recipe and preparation of these slurries is similar to the original anode slurry, processed in the decanter centrifuge, with only the respective volume fractions of the missing or reduced particle component being substituted by deionized water. As the measurement of all prepared anode slurries with the analytical methods used are only possible at lower solid volume fractions, a subsequent dilution of the concentrated slurries with deionized water is carried out, which differs depending on the method.

2.3. Analytical instruments and methods

To evaluate the fractionation of the aqueous slurry into graphite and carbon black in the decanter centrifuge, graphite and carbon black concentrations in aqueous samples must be determined. Graphite particles have a larger particle size compared to carbon black particles, which is already indicated by the SEM images in Fig. 1 and later illustrated in Fig. 2, showing the different particle size distributions of the two materials in aqueous phase. The different particle sizes and densities (1600 kg/m^3 for carbon black and 2200 kg/m^3 for graphite) also cause significantly different sedimentation velocities of the single particles of the two materials. This becomes clear when considering Stokes' law [28], describing the sedimentation velocity v_s of a spherical single particle in a stationary Newtonian fluid at small Reynolds numbers without mutual particle interference (see Equation (1)).

$$v_s = \frac{(\rho_s - \rho_f)\cdot a \cdot x^2}{18\cdot \eta_f} \tag{1}$$

In addition to the fluid density ρ_f, fluid viscosity η_f, and centrifugal acceleration a, the particle density ρ_s and size x affect the sedimentation velocity. The higher density and size of graphite particles thus result in significantly higher sedimentation velocities of the single particles in liquid phase compared to carbon black. With a laser diffraction instrument and the LUMiSizer©, two analytical instruments are available offering the potential to differentiate the materials based on the different particle sizes and sedimentation velocities in the centrifugal field. The two analytical instruments, their measurement methods developed for this application, and the characterization of the individual materials using the two instruments as reference measurements are presented below.

Before the methods can be used for this application, it is necessary to do preliminary tests. For this purpose, measurements of defined anode slurries with reduced graphite and carbon black fractions compared to the original anode slurry were carried out using both methods. The fraction of one of the two solid components remains constant in this slurry compared to the original anode slurry, while the fraction of the other component is varied. The composition of the anode slurries are described in this work by the parameters ϕ_g for graphite and ϕ_{cb} for carbon black. While ϕ_g indicates the ratio between the volume fraction of graphite particles in the present anode slurry $c_{v,g}$ and in the original

slurry $c_{v,g,0}$ (see Equation (2)), ϕ_{cb} represents the ratio between the volume fraction of carbon black particles in the present anode slurry $c_{v,cb}$ and in the original slurry $c_{v,cb,0}$ (see Equation (3)). This means, in a slurry with ϕ_g of 20 % as an example, only 20 % of the graphite volume fraction in the original anode slurry is left in the present slurry.

$$\phi_g = \frac{c_{v,g}}{c_{v,g,0}} \cdot 100\% \quad (2)$$

$$\phi_{cb} = \frac{c_{v,cb}}{c_{v,cb,0}} \cdot 100\% \quad (3)$$

The measurements are used to investigate the detection limit of the different components. They also serve as a reference for the application of the measurement methods to anode slurries whose composition is unknown after the fractionation step in the decanter centrifuge. By comparing the measurement results of the sample with unknown composition with the reference measurements of the anode slurries with different graphite and carbon black fractions, an estimation of the component fractions in the sample is possible. Table 1 gives an overview of the studied variations of the volume fractions of graphite and carbon black in a carbon-black-rich or graphite-rich slurry for both analytical methods.

2.3.1. Particle size analysis by laser diffraction

Particle size distributions of aqueous samples were measured with the HELOS H0309 laser diffraction instrument (Sympatec GmbH). For the measurement, a dilution of the sample with deionized water to a solid volume fraction in the range of 10^{-5} to 10^{-6} is necessary to achieve an optical concentration of about 20 %.

Figure 2 shows the volume-weighted cumulative particle size distribution $Q_3(x)$ of an original anode slurry, a pure carbon black slurry, and a pure graphite slurry measured with the laser diffraction instrument. The volume-weighted cumulative particle size distribution $Q_3(x)$ represents the volume fraction of particles smaller than the certain particle size x related to the total particle volume. Graphite particles have a mean particle size $x_{50,3}$ of 21.2 µm. This means that graphite particles smaller than 21.2 µm occupy 50 % of the total particle volume. The parameter *span*, which is the difference between $x_{90,3}$ and $x_{10,3}$ related to $x_{50,3}$, describes the width of the particle size distribution (see Equation (4)). Particles whose particle size is smaller than the value of $x_{10,3}$ or $x_{90,3}$ exhibit a volume fraction of 10 or 90 %,

$$span = \frac{x_{90,3} - x_{10,3}}{x_{50,3}} \quad (4)$$

The *span* for graphite is comparatively low at 0.9, which is why a narrow particle size distribution can be assumed here. The mean particle size $x_{50,3}$ of the agglomerated carbon black particles is 4.4 µm and they are more widely distributed (*span* = 3.2). Graphite particles are distributed over a coarse particle size range, while carbon black particles are mainly in a finer particle size range. There is only an overlap range between about 7 and 23 µm, where 30 vol% of the carbon black particles are in the size range of graphite particles. As expected, the original anode slurry with both materials shows a bimodal particle size distribution characterized by the bend in the distribution. However, the significant differences in the particle size distributions between the two materials allow the fractions of carbon black and graphite in an aqueous anode slurry to be estimated by particle size analysis using laser diffraction.

Table 1
Studied variations of the volume fractions of graphite and carbon black in a carbon-black-rich or graphite-rich slurry for both analytical methods.

	Particle size analysis by laser diffraction	Sedimentation analysis with the LUMiSizer©
ϕ_g / %	25, 10, 1	50, 33, 25, 20, 10
ϕ_{cb} / %	25, 10, 1	20, 10, 2, 1

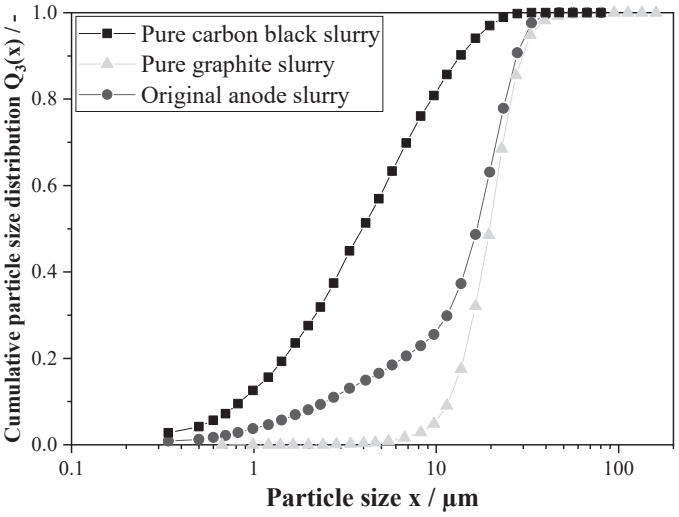

Fig. 2. Cumulative particle size distributions of a pure carbon black and graphite slurry determined by HELOS H0309 laser diffraction instrument (Sympatec GmbH).

2.3.2. Sedimentation analysis by the LUMiSizer©

The analytical centrifuge LUMiSizer© (LUM GmbH) was used to analyze the sedimentation behavior of the particles in liquid phase in the centrifugal field. After filling the sample into the cuvette, the sample is centrifuged with simultaneous exposure to monochromatic light with a wavelength of 870 nm over the entire length of the cuvette. The particles cause a characteristic extinction of the light and the corresponding transmission profiles of the light are recorded as a function of time by charge-coupled device (CCD) detectors. The analysis software SEP-View© calculates sedimentation velocities of the particles in the sample from the temporal transmission changes. A detailed description of the measurement principle can be found in Lerche [41].

As a result of the lower density and particle size of the carbon black particles compared to the graphite particles, considerably lower sedimentation velocities can be expected for carbon black in the centrifugal field. On the one hand, these differences are the basis for the separation process of the anode slurry into graphite and carbon black in the decanter centrifuge. On the other hand, these differences can also be used to determine carbon black and graphite fractions by analyzing the particle sedimentation velocity distribution of an aqueous anode slurry sample with the LUMiSizer©.

To obtain a complete sedimentation velocity distribution of the entire graphite and carbon black particles in the sample, some requirements have to be fulfilled. The solid volume fraction of the sample has to be adjusted in such a way that changes of the transmission profiles over time are still detectable and there is as low as possible mutual interference of the particles during sedimentation. If the solid volume fraction is too high, the light is strongly attenuated or absorbed by the particles that no transmitted light is detected. The high light absorption is a problem especially for the very dark to black graphite and carbon black particles at high solid volume fractions. With rising particle content, mutual particle interference increases during sedimentation, resulting in a broad settling velocity distribution or the formation of a zone settling regime in the worst case, making it difficult to distinguish between graphite and carbon black particles by applying this measurement method. Furthermore, a complete detection of the entire settling particles up to the deposition at the bottom of the cuvette in the measurement time and thus the selection of an appropriate centrifugal acceleration are important. On the one hand, the centrifugal acceleration should be as high as possible so that even very fine carbon black particles

can be completely deposited in a practicable measurement time. On the other side, if the centrifugal acceleration is too high, there is a risk that especially coarse graphite particles have very high sedimentation velocities and thus their sedimentation cannot be detected even at the lowest measurement interval.

A two-stage sedimentation analysis with the LUMiSizer© fulfills these requirements. In the first stage, mainly coarse graphite and carbon black particles are completely deposited and detected at a low centrifugal acceleration of 9 g for 5 min. A transmission profile is recorded every second. For a complete deposition and recording of very fine graphite and carbon black particles, a centrifugation at a centrifugal acceleration of 2325 g is carried out for 2 h at a measuring interval of 10 s in the second stage. As an evaluation of the particle settling velocities is no longer comparable due to the different centrifugal accelerations, the analysis in SEPView© is performed with a method considering the different centrifugal accelerations where the transmission profiles were recorded. The method analyzes the cumulative intensity distribution over the equivalent particle size calculated from the sedimentation velocity according to Stokes [28]. As the specification of a solid density is necessary for this calculation, the determined particle size is only an equivalent particle size. The solid density specified was that of graphite. As the measurement and evaluation method should only estimate graphite and carbon black fractions in an aqueous slurry and not a particle size distribution, this circumstance is not relevant for this application. For the sedimentation analysis of an aqueous anode slurry sample, a high dilution to a solid volume fraction of 0.110 % for an expected graphite-rich slurry and 0.012 % for an expected carbon-black-rich slurry is necessary.

Figure 3 shows the cumulative intensity distribution over the equivalent particle size for the original anode slurry with a total solid volume fraction of 0.122 %, a pure graphite slurry with a solid volume fraction of 0.110 %, and a pure carbon black slurry with a solid volume fraction of 0.012 %. The solid volume fractions of the pure slurries correspond to the respective volume fraction of the component in an original anode slurry diluted for the sedimentation analysis. The distributions of the two pure slurries differ significantly from each other. Only a small overlap area between coarse carbon black particles and fine graphite particles can be seen. For the distribution of the pure graphite slurry, a sharp bend is noticeable at an equivalent particle size of 2 µm. This bend is caused by the change of the centrifugal acceleration from 9 to 2325 g, resulting in the deposition of a very fine particle fraction of graphite particles, which is significantly different from the remaining graphite particles in terms of particle size. Since only few or no particles

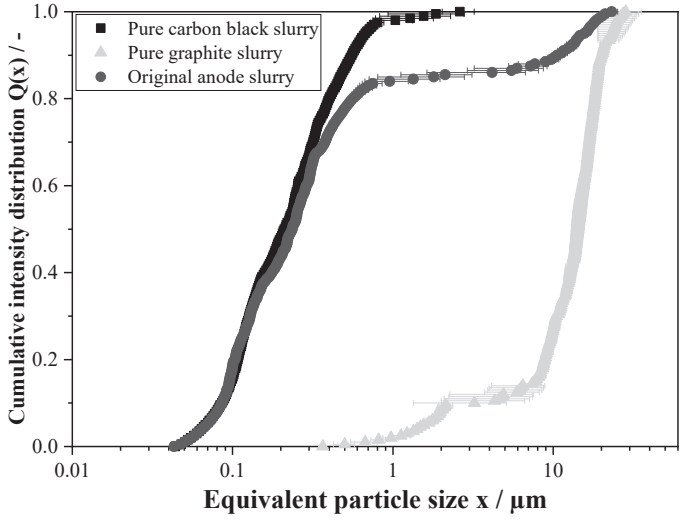

Fig. 3. Cumulative intensity distribution of a pure carbon black and graphite slurry measured by LUMiSizer© (LUM GmbH).

in this size range are detected in the particle size distribution of pure graphite measured with the laser diffraction instrument (see Fig. 2), it can be assumed that the volume fraction of these very fine particles in the graphite material is negligible. The distribution of the original anode slurry with both materials is bimodal and lies between the distributions of the pure materials. Basically, the described sedimentation analysis with the LUMiSizer© is suitable to estimate graphite and carbon black fractions in an aqueous slurry with unknown composition, considering the significantly different measured cumulative intensity distributions of the two pure materials. As with particle size analysis by laser diffraction, this requires reference measurements of anode slurries with defined graphite and carbon black fractions, which also are used to determine the detection limit of the method.

2.4. Centrifugal fractionation in the decanter centrifuge

The fractionation of the anode slurry into the active material graphite and the conductive additive carbon black was carried out in the continuous pilot-scale decanter centrifuge MD 80 (Lemitec GmbH). The setup of the decanter centrifuge and the ideal fractionation of the anode slurry, as expected in the apparatus based on the different physical properties of graphite and carbon black particles, is shown in Fig. 4.

The apparatus consists of a cylindrical-conical drum enclosing a screw conveyor. As the drum rotates, centrifugal forces act on the suspension. As a result of the density difference between graphite and water, graphite particles settle on the drum wall and form a sediment. The screw conveyor rotates at a higher speed to the drum and conveys the settled graphite particles out of the centrifuge. At the same time, a liquid level is formed on the drum wall, whose height is adjusted by an overflow weir. A major part of the water flows with the carbon black particles along the screw winding to the cylindrical drum end and drains off over the overflow weir. As carbon black particles have only low settling velocities compared to graphite due to their low density difference to water and their particle size, the residence time in the centrifuge is not sufficient to deposit the particles on the drum wall. Thus, a fractionation of the aqueous anode slurry into graphite particles in the sediment and carbon black in the centrate happens in the best case.

Fractionation of the aqueous anode slurry in the decanter centrifuge was carried out at a constant differential speed between the screw and the drum of 20 min^{-1} and a liquid level of 10 mm. The peristaltic pump Verder 2006 Auto High Flow Pump (Verder Deutschland GmbH & Co. KG) supplies the slurry feed to the decanter centrifuge at varying volumetric flows of 23, 43, and 66 l/h from a 30 l vessel. The agitator system Heidolph RZR 50 (Heidolph Instruments GmbH & Co. KG) ensures the mixing of the slurry in the vessel at a speed of approx. 600 rpm. The centrifugal accelerations investigated were 352 and 626 g, which corresponds to a speed of the centrifuge drum of 3000 and 4000 rpm. To determine the success of the fractionation process, it is necessary to analyze graphite and carbon black fractions in the centrate and sediment. For this purpose, centrate and sediment samples are taken and diluted before the sedimentation analysis with the LUMiSizer© (see Chapter 2.3.2) and the particle size analysis by laser diffraction (see Chapter 2.3.1) can be applied. Samples for the analysis by laser diffraction are diluted until an optical concentration of approx. 20 % is reached. Before using the sedimentation analysis, the solid volume fraction of the sample is measured by drying for about 24 h at 50°C in an oven and gravimetric analysis of the sample before and after drying to determine the water volume to be added for the required dilution. As it is assumed that the centrate contains only carbon black particles and the sediment consist of only graphite particles, the centrate sample is diluted to 0.012 % solid volume fraction of a pure carbon black slurry and the sediment sample to the 0.11 % solid volume fraction of a pure graphite slurry, as in the reference measurements in Fig. 3.

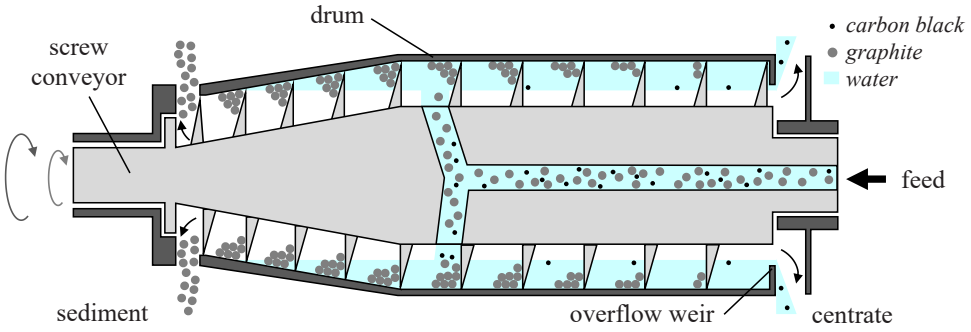

Fig. 4. Schematic illustration of the fractionation of an anode slurry into graphite and carbon black in a decanter centrifuge.

3. Results and discussion

3.1. Testing of the analytical methods for the determination of graphite and carbon black fractions in aqueous slurries

3.1.1. Particle size analysis by laser diffraction

In Fig. 5, the particle size distributions determined by the laser diffraction instrument of the pure graphite slurry, the pure carbon black slurry, and the anode slurry with constant carbon black fraction and varying graphite fractions are presented.

As expected, the particle size distributions of the anode slurry with constant carbon black fraction and reduced amount of graphite compared to the original anode slurry are between the distributions of the pure carbon black and original anode slurry. With decreasing amount of graphite, the distribution of the anode slurry approaches the distribution of a pure carbon black slurry. The distribution of the mixture with the lowest graphite fraction of 1 % is almost congruent with the distribution of the pure carbon black slurry, while the distributions of the mixtures with graphite fractions of 25 % and 10 % clearly differ from that of pure carbon black. Also, for the fractions of 25 % and 10 %, there is still a bend in the disbtribution as for the original anode slurry, signifying the bimodality of the distribution and clearly demonstrating the presence of graphite particles in the mixture. On the contrary, with a graphite fraction of 1 %, no bend in the distribution and thus no bimodality can be seen. This means that a clear detectability of such a low graphite fraction in an anode slurry with the analytical method is no longer given. It is expected that carbon black particles almost completely get into the centrate flow leaving the decanter centrifuge, while graphite particles are mainly deposited and thus only minor graphite impurities are found in the centrate flow. Thus, the reference measurements shown with constant carbon black fraction and reduced graphite fractions are suitable for estimating the composition of centrate samples to assess the fractionation effect in the decanter centrifuge. With the method, down to 10 % of graphite particles getting into the centrate or up to 90 % graphite separation efficiency in the centrifuge can be detected.

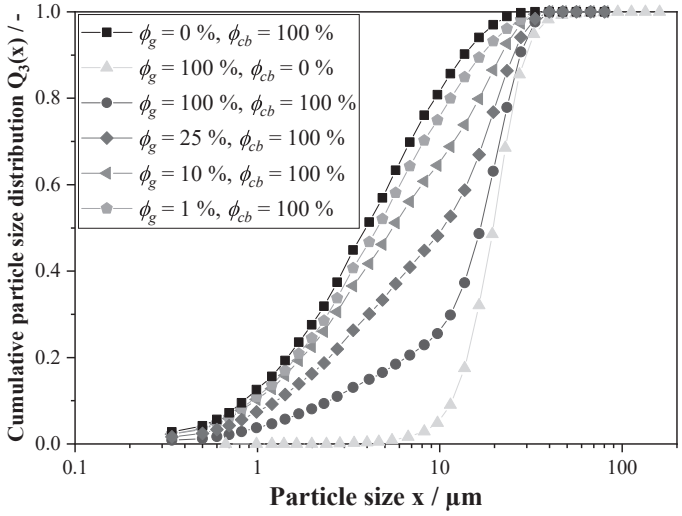

Fig. 5. Cumulative particle size distributions of pure graphite, pure carbon black, and anode slurries with varying amounts of graphite.

The particle size distributions of anode slurry with constant amount of graphite and decreased carbon black fractions are compared with those of pure graphite, pure carbon black, and the original anode slurry in Fig. 6. It can be observed that the particle size distributions of the anode slurries shift to the right towards the distribution of a pure graphite slurry with decreasing carbon black fractions. At 1 % carbon black fraction, the distribution is almost exactly on the distribution of the pure graphite slurry. At carbon black fractions of 25 % and 10 %, carbon particles can be clearly identified based on the higher amount of fine particles in the distribution compared to the pure graphite slurry. The instrument also detects particles in the size range smaller than 2 µm for these two anode slurries. This particle size range is characteristic for carbon black particles, since graphite does not consists of such small particles and they can only be found in pure carbon black. At 1 % carbon black in the anode slurry, the distribution does not contain particles smaller than 2 µm. The mixtures with constant graphite fraction and reduced carbon black fraction imitate the sediment in the decanter centrifuge, where mainly graphite with low carbon black impurities can be expected according to the different separation behavior of the two components in the centrifugal field. Thus, the particle size distributions of these mixtures are a useful reference for the measured distributions of sediment samples with unknown composition to determine separation efficiencies of carbon black greater than 10 %.

3.1.2. Sedimentation analysis with the LUMiSizer©

Figure 7 displays the cumulative intensity distributions determined by the LUMiSizer© for pure carbon black, pure graphite, and anode slurries with constant carbon black fraction and varying graphite fractions.

Similar to the particle size analysis, the distributions of anode slurries with varying graphite fractions lie between that of pure carbon black and the original anode slurry and converge to the distribution of pure carbon black as the graphite fraction decreases. The level of the characteristic bend in the distribution caused by the graphite particles increases with reduced graphite fraction. The distribution at a graphite fraction of 25 % is almost identical to the distribution of pure carbon black. However, the only difference to the distribution of pure carbon black is that the distribution still extends slightly into the equivalent particle size range larger than 3 µm, which can clearly be assigned to graphite particles. With a graphite fraction of 20 %, no differences to the distribution of pure carbon black can be observed within the standard deviations. Thus, only graphite fractions down to 25 % compared to the original anode slurry, corresponding to graphite separation efficiencies

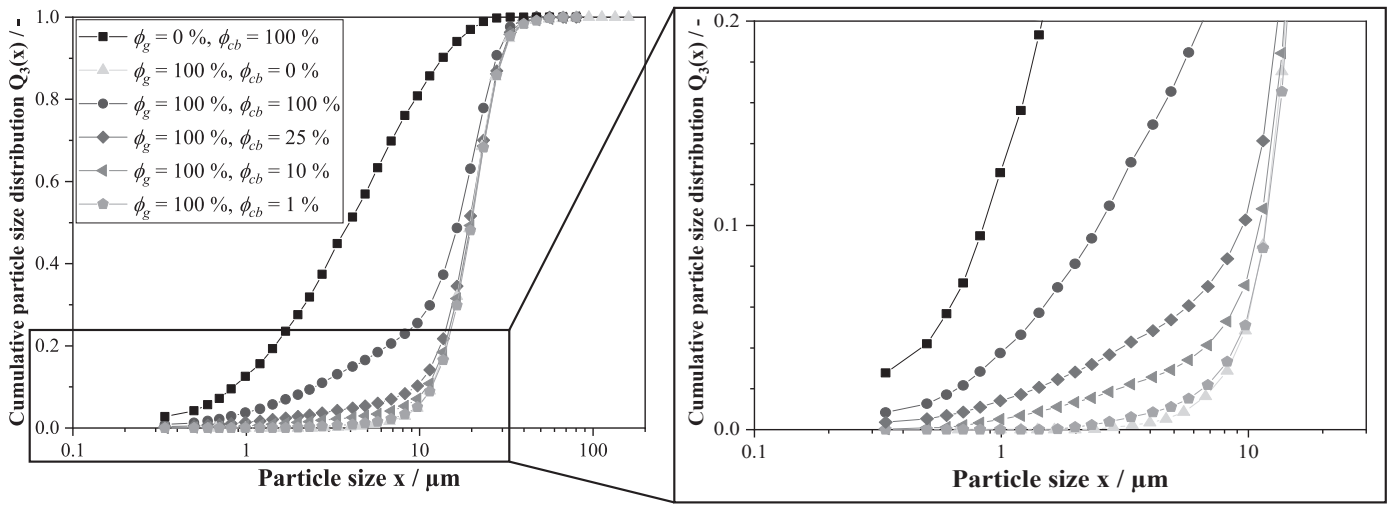

Fig. 6. Cumulative particle size distributions of pure graphite, pure carbon black, and anode slurries with varying amounts of carbon black.

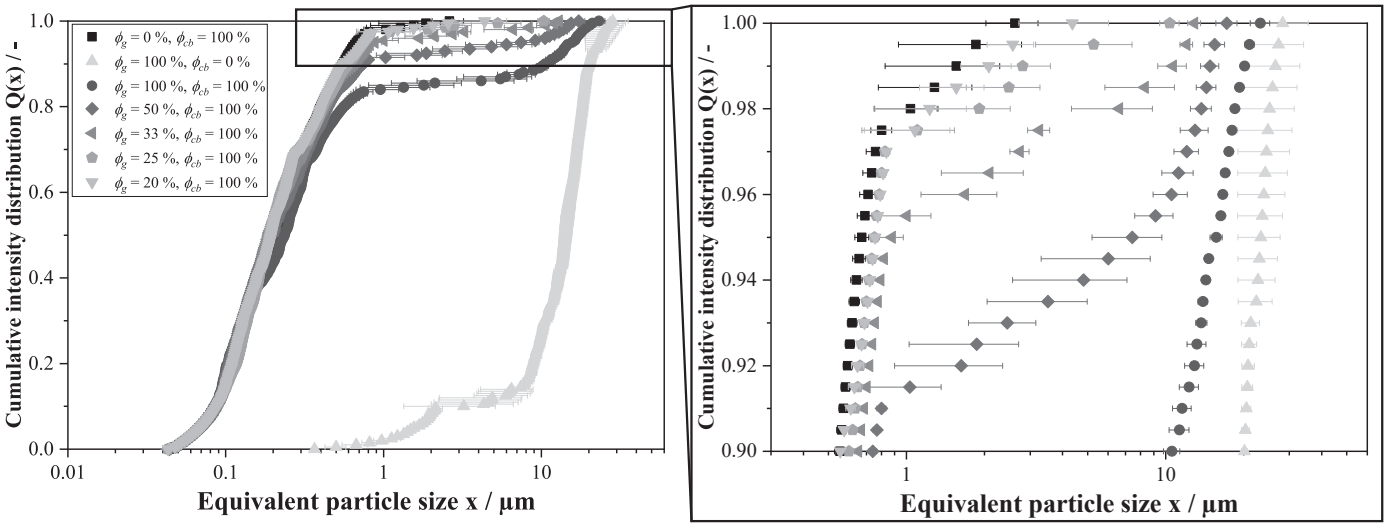

Fig. 7. Cumulative intensity distributions of pure graphite, pure carbon black, and anode slurries with varying amounts of graphite.

up to 75 %, can be detected in centrate samples with constant carbon black fraction by the sedimentation analysis.

To improve the detectability of graphite particles in carbon-black-rich centrate samples, the concentrating method illustrated in Fig. 8 was developed. In the best case, the centrate should contain only carbon black particles in the fractionation process of an anode slurry in the decanter centrifuge. However, in reality, it is possible that graphite particles could also be present in the centrate, which needs to be analyzed by the analytical methods. Therefore, the concentrating method is shown in Fig. 8 for a centrate sample containing mainly carbon black particles with a small fraction of graphite particles as an example. The method targets to enrich graphite particles from a centrate sample in the cuvette of the LUMiSizer©. First, the cuvette is filled with twice of the usual sample volume needed for a measurement with the

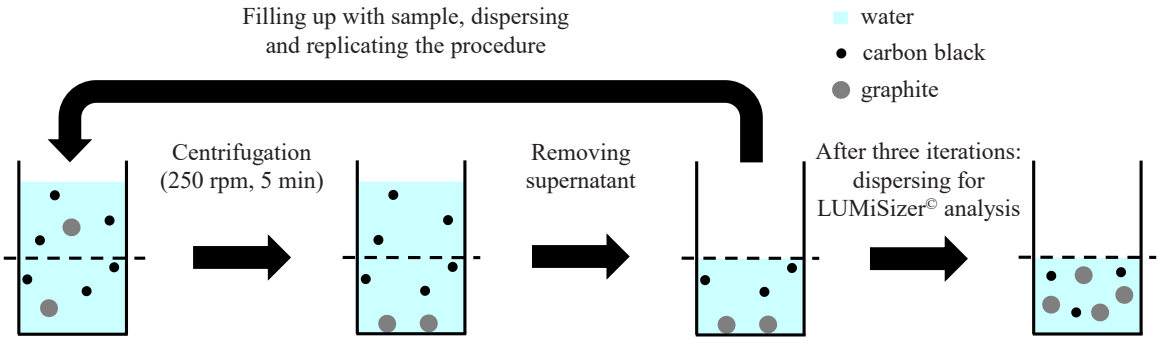

Fig. 8. Schematic illustration of the concentrating method for a centrate sample containing mainly carbon black particles and minor impurities of graphite as an example.

sedimentation analysis. This is followed by a centrifugation of the sample at 9 g for 5 min. The centrifugal acceleration and time chosen correspond to those in the first cycle of the usual sedimentation analysis with the LUMiSizer©, where a complete separation of graphite particles is expected. However, carbon black particles remain homogeneously distributed in the supernatant under these centrifugation conditions and are not deposited. The upper half of the sample volume is removed as part of the supernatant to fill the removed volume with further centrate sample. After the sample is subsequently dispersed, the procedure is repeated to further increase the graphite concentration in the sample. After three iterations, the graphite concentration is increased by a factor of 3 from initial 10–30 % of the graphite volume in the original anode slurry, while the carbon black concentration in the sample remains constant. Finally, the usual sedimentation analysis by the LUMiSizer© is applied to the sample. The iterative sample dispersion is essential to minimize the small amount of coarse carbon black particles that may have also settled during the low centrifugal acceleration.

The known intensity distributions of pure carbon black, pure graphite, and the original anode slurry are shown in Fig. 9. In addition, the intensity distributions of an anode slurry with a constant carbon black fraction and graphite fraction of 10 % and a pure carbon black slurry, both treated with the previously described concentrating method before the sedimentation analysis, can be seen in Fig. 9. Despite the use of the concentrating method, the distribution of the pure carbon black slurry is almost identical to that which was not treated with the concentrating method. Only a slight shift of the distribution to the right in the range between 0.7 and 1 towards a bit higher equivalent particle sizes can be noticed. This can be explained by the deposition of a few coarse carbon black particles during the concentrating method. Since the shift in the distribution does not extend into the characteristic equivalent particle size range of graphite, this confirms the basic suitability of the method to unambiguously detect low concentration graphite in anode slurries. For the anode slurry with 20 % graphite fraction, no clear differentiation from the distribution of the pure carbon black slurry and thus graphite detection could be established without the concentrating method (see Fig. 7). However, a clearly different distribution is obtained for the anode slurry with a graphite fraction of 10 % by using the concentrating method, which extends from 0.98 into the equivalent particle size range larger than 3 µm, which is only typical for graphite, and thus clearly provides evidence of graphite particles in the slurry. Finally, it can be stated that an enhancement of the graphite detection limit is possible with the concentrating method before the sedimentation analysis with the LUMiSizer©. Thus, graphite separation efficiencies up to 90 % can be detected by applying this analytical method to centrate samples.

To investigate the limit of the method for detecting carbon black in graphite-rich anode slurries existing in the case of sediment samples, the intensity distributions of pure carbon black, pure graphite, and anode slurry with constant graphite fraction and varying carbon black fraction are presented in Fig. 10. As expected, the distributions of the anode slurry with reduced carbon black fraction are between the distribution of pure graphite and the original anode slurry. If the carbon black fraction in the anode slurry decreases, the distribution approaches that of pure graphite. The height of the characteristic transition area between carbon black and graphite particles, which drops with decreasing carbon black fraction, is a suitable indicator for the carbon black fraction contained in a graphite-rich slurry. In the equivalent particle size range smaller than 0.4 µm, which is characteristic only for carbon black particles, carbon black particles are still clearly detectable for all anode slurries down to a very low carbon black fraction of only 1 %. The method can thus detect carbon black separation efficiencies down to 1 % based on analyzing sediment samples.

Table 2 summarizes the limit fractions of graphite in a carbon black-

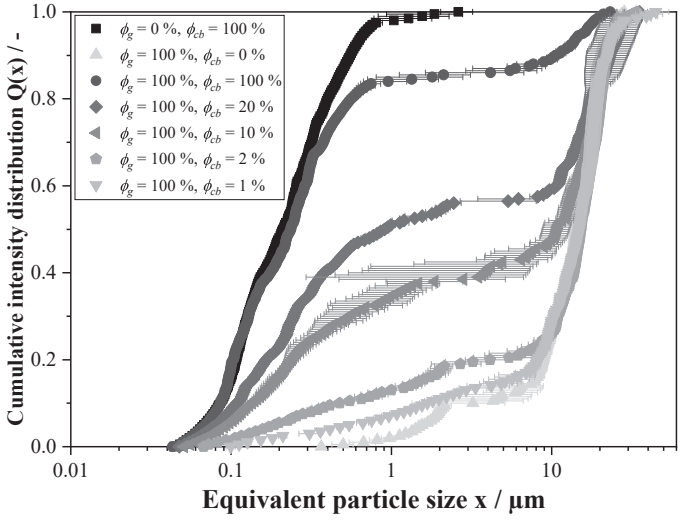

Fig. 10. Cumulative intensity distributions of pure graphite, pure carbon black, and anode slurries with varying amounts of carbon black.

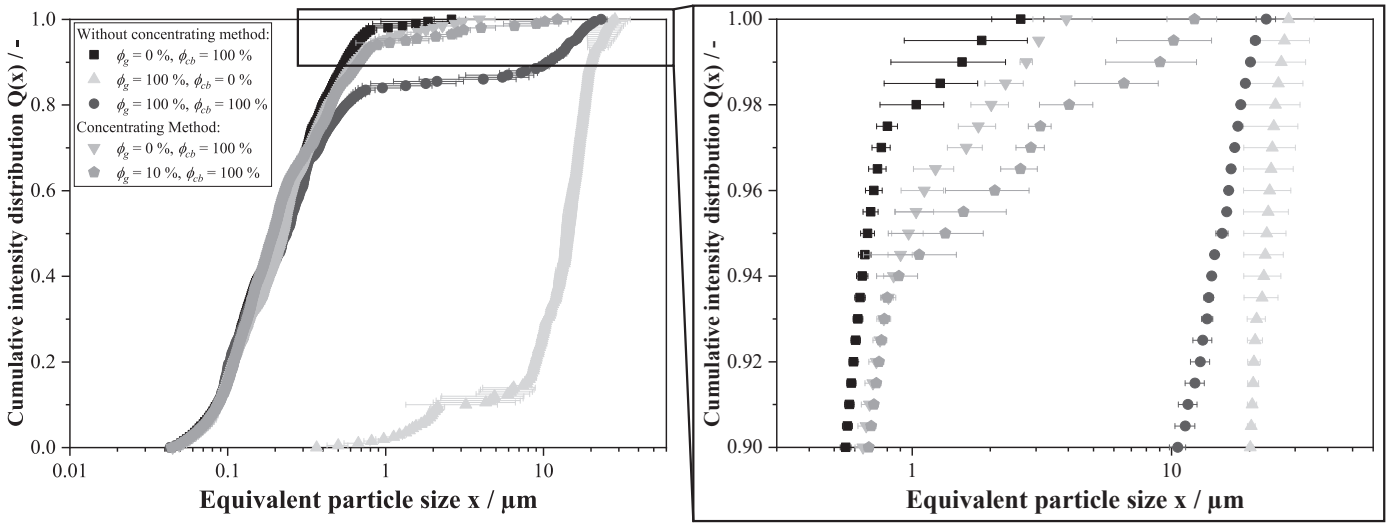

Fig. 9. Cumulative intensity distributions of pure graphite, pure carbon black, original anode slurry, and anode slurry with constant carbon black content and 10 % graphite content handled with and without the concentrating method.

Table 2
Detection limits of graphite (ϕ_g) in a carbon-black-rich sample (centrate) and carbon black (ϕ_{cb}) in a graphite-rich sample (sediment) for the analytical methods.

	ϕ_g / %	ϕ_{cb} / %
Particle size analysis	10	10
Sedimentation analysis without concentrating method	25	1
Sedimentation analysis with concentrating method	10	–

rich sample and carbon black in a graphite-rich sample that can be still clearly detected by the particle size analysis and the sedimentation analysis. The detection limit of 25 % graphite fraction is less deep for the sedimentation analysis without the concentrating method than for the particle size analysis, which can detect graphite fractions down to about 10 %. With the concentrating method before the sedimentation analysis, the detection limit is improved down to a graphite fraction of 10 %, which can keep up with that of the particle size analysis. Maybe more iteration steps in the concentration method could increase the detection limit of the sedimentation analysis. The detection limit of carbon black in a graphite-rich anode slurry is significantly lower than the detection limit of graphite in a carbon-black-rich anode slurry for the sedimentation analysis. This indicates that carbon black particles cause significantly higher light extinction compared to graphite particles. As carbon black particles have significantly smaller particle sizes than graphite, the volume-specific surface area of carbon black particles is larger than graphite. The light extinction of the particles increases with rising volume-specific particle surface, resulting in a significantly higher detectability of carbon black by the method than graphite. Also, carbon black particles can be measured at significantly lower concentrations in sediment samples with the sedimentation analysis compared to the particle size analysis.

3.2. Fractionation of an aqueous anode slurry in the decanter centrifuge

3.2.1. Evaluation by the LUMiSizer© sedimentation analysis

In Fig. 11 the cumulative intensity distributions of centrate samples taken after fractionation experiments in the decanter centrifuge at a constant centrifugal acceleration of 352 g and different feed volume flows can be found. The reference measurements of pure graphite, pure carbon black, the original anode slurry, and a defined anode slurry with a reduced graphite fraction of 10 % are also plotted for comparison. Similar to the measurements of pure carbon black and the anode slurry with a reduced graphite fraction of 10 %, the concentrating method was also applied to the centrate samples.

It can be seen that the distributions of all centrate samples approximately coincide with the distribution of pure carbon black. The reference measurement of an anode slurry with 10 % graphite fraction, representing the detection limit of graphite in carbon-black-rich slurries, deviates above about 0.98 into the characteristic equivalent particle size range larger than 3 µm. No particles are found in the centrate samples in this range. These circumstances indicate that a high graphite deposition of at least 90 % is present. Compared to the samples taken at the higher feed volume flows of 43 and 66 l/h, the distribution of the centrate sample at 23 l/h is shifted slightly to the left towards that of pure carbon black. A lower volume flow increases the residence time of the particles in the decanter centrifuge, resulting in more particles being deposited. Since this shift is in the equivalent particle size range where fine graphite and coarse carbon black particles overlap, and the distribution is even slightly to the left away from the carbon black distribution, increased deposition of both materials is possible.

Figure 12 compares the reference measurements with the centrate samples at a higher centrifugal acceleration of 626 g and different volume flows. The distributions of the centrate samples correspond to the reference measurement of pure carbon black and no particles with an equivalent particle size in the characteristic graphite range larger than 3 µm are detected. Thus, a high graphite separation of at least 90 % can also be assumed here. While particles with an equivalent particle size between approx. 2.7 and 3 µm are still present in the distribution of pure carbon black, this is not the case for the centrate samples and their distributions are further to the left. The reason for this is that coarse carbon black particles are also deposited at this higher centrifugal acceleration. Overall, the distributions of the centrate samples are shifted slightly further to the left compared to the low centrifugal acceleration, suggesting higher particle deposition due to the higher centrifugal forces acting on the particles. It is concluded that the graphite separation can be estimated to be at least 90 % for the entire operation conditions investigated.

Figure 13 shows the cumulative intensity distributions of the sediment samples taken at the same operation conditions as the centrate samples. Also the cumulative intensity distributions of pure graphite, pure carbon black, the original anode slurry, and anode slurries with reduced carbon black fraction are given as a reference. The distributions of the three measurements are shown separately for some sediment samples instead of as mean values with corresponding standard deviations. That is caused by the fact that the distributions differ especially

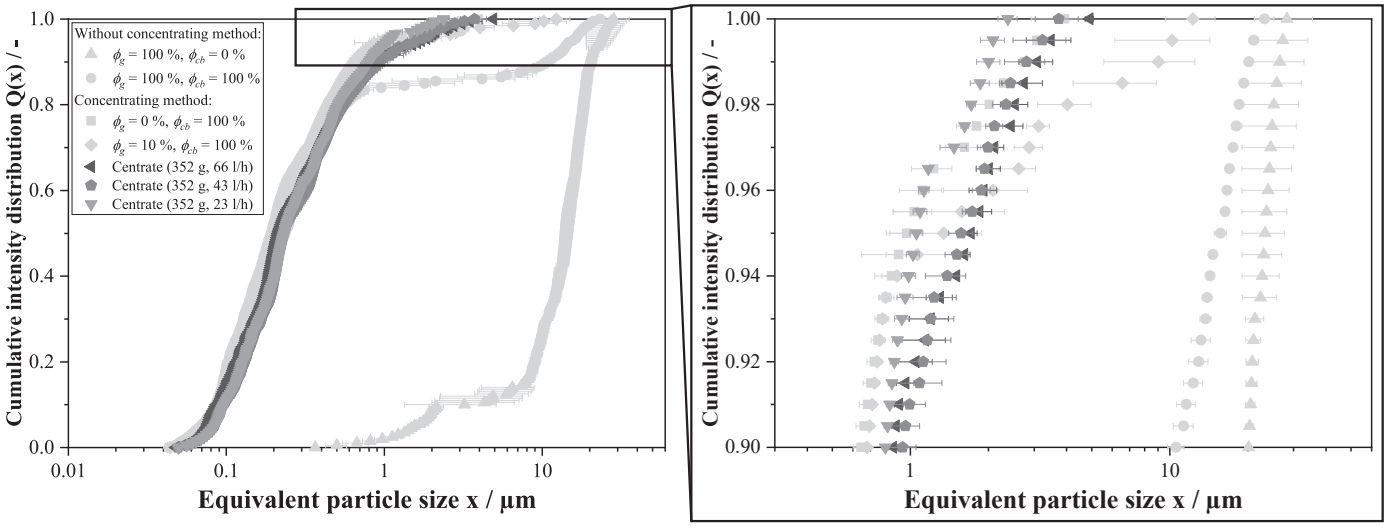

Fig. 11. Cumulative intensity distributions of reference measurements determined with and without the concentrating method and centrate samples taken at a constant centrifugal accelerations of 352 g and different volume flows from the decanter centrifuge.

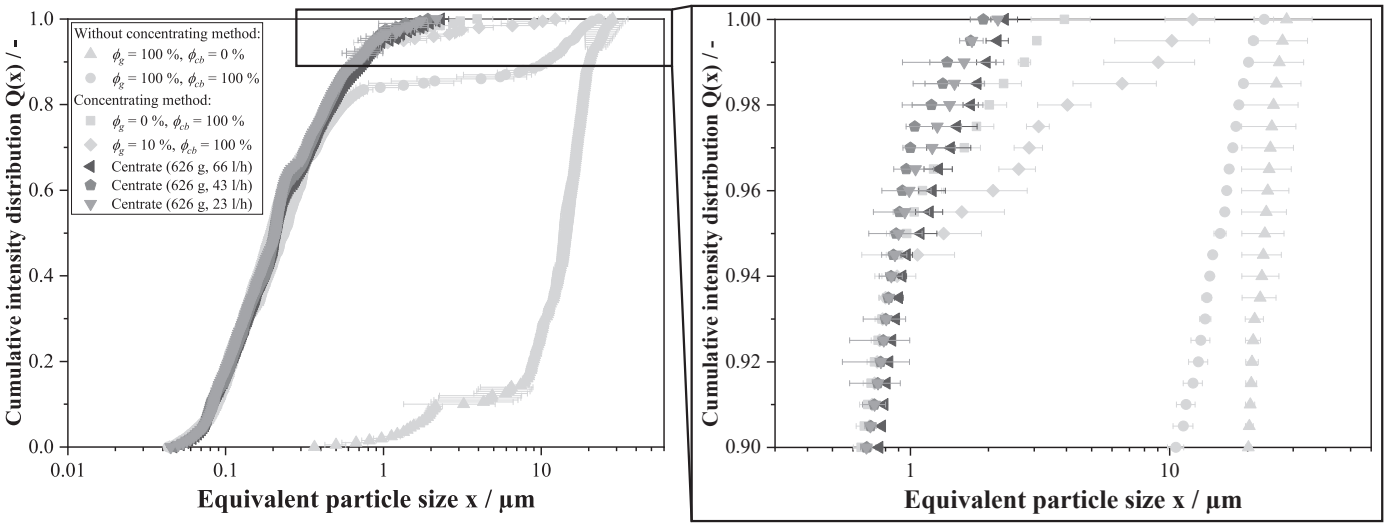

Fig. 12. Cumulative intensity distributions of reference measurements determined with and without concentrating method and centrate samples taken at a constant centrifugal accelerations of 626 g and different volume flows from the decanter centrifuge.

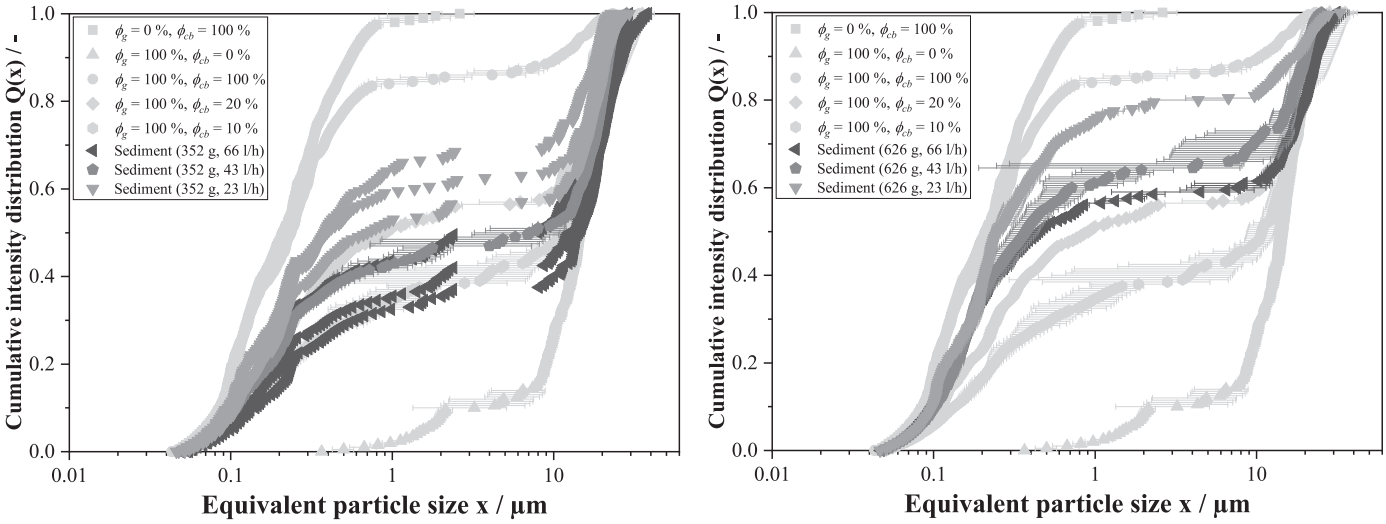

Fig. 13. Cumulative intensity distributions of reference measurements and sediment samples taken at different centrifugal accelerations and different volume flows from the decanter centrifuge.

in the level of the transition area, indicating the fraction of carbon black in the sample. For example, for a centrifugal acceleration of 352 g at a volume flow of 66 l/h, two measurements are almost congruent with the reference measurement with a carbon black fraction of 10 %, while the third measurement is in the range between the reference measurements with 10 % and 20 % fraction. Although the deviation of the carbon black fraction between the measurements is not very high, this small difference has a significant effect on the standard deviations of the equivalent particle size in the transition area of the distribution.

The carbon black separation efficiency at 352 g and 66 l/h is thus approximately between 10 % and 20 %. The distribution of the sediment for a feed volume flow of 43 l/h at the same centrifugal acceleration is also exactly between the reference measurements of 10 % and 20 % carbon black fraction. In contrast, the distributions of the sediment sample at the lowest feed volume flow tested of 23 l/h, representing the highest residence time of particles in the decanter centrifuge, are either exactly at or above the reference measurement of 20 % carbon black fraction. It is clear that the carbon black fraction in the sediment or the carbon black separation efficiency increases with lower volume flow or higher residence time, as expected. The effect is found again at the higher centrifugal acceleration of 626 g. The distributions of the sediment deviate to a greater extent upward from the reference measurement at a carbon black fraction of 20 % with decreasing volume flow or increasing residence time. Compared to the distributions at the lower centrifugal acceleration of 352 g at the same volume flow, the levels of the transition area are higher in all cases at the higher centrifugal acceleration. The higher the centrifugal acceleration at the same volume flow is, the more carbon black particles are deposited and end up in the sediment. Increasing the volume flow or the centrifugal acceleration leads to a higher graphite deposition, as can be seen from the centrate samples in Figs. 11 and 12. On the other hand, this also results in significantly more carbon black particles getting into the sediment, as revealed by the sedimentation analysis of the sediment sample. Furthermore, it is noticeable that particles over almost the entire equivalent particle size range, which is unique to carbon black, are basically found in all sediment samples. Even very fine carbon black particles, whose deposition is expected rather at higher centrifugal accelerations and residence times, are found in the sediment. As the considered solid volume fraction of the fed anode slurry is relatively high, mutual particle influence during the sedimentation process can be

assumed [39,40]. Fine carbon black particles are thus dragged into the sediment by settling coarse carbon black or graphite particles or by the formation of heteroagglomerates.

3.2.2. Evaluation by particle size analysis measured with laser diffraction

Particle analysis by laser diffraction instrument was applied only to centrate and sediment samples at sporadic operating conditions, mainly to validate the results of the sedimentation analysis with the LUMiSizer©, which has a deeper detection limit of carbon black in graphite-rich slurries. The particle size distribution of centrate samples taken at centrifugal acceleration of 626 g and two volume flows of 23 and 66 l/h are given in the Fig. 14 together with the corresponding reference measurements.

The distribution of the centrate sample at the low volume flow rate of 66 l/h lies between the distribution of pure carbon black and the anode slurry with a graphite fraction of 10 %, which is the detection limit of graphite in a carbon-black-rich anode slurry, as in the sedimentation analysis with the LUMiSizer. The distribution of the centrate sample at the lower flow rate of 23 l/h matches exactly the distribution of pure carbon black. In both cases, at least 90 % of the graphite particles are separated. However, the graphite separation efficiency of the lower flow rate of 23 l/h can be estimated to be higher, as the distribution is closer to the distribution of pure carbon black than the distribution of the centrate sample at 66 l/h. Considering the higher residence time at a lower volume flow which gives the particles more time to be separated in the decanter centrifuge, this observation is not surprising.

Figure 15 displays the particle size distributions of the equivalent sediment samples at the same operation parameters and the corresponding reference measurements. The distribution of the sediment at a volume flow of 66 l/h is between the distributions of an anode slurry with 10 % and 25 % carbon black fraction, indicating a carbon black separation efficiency between 10 % and 25 %. As the particle size distribution of the sediment sample at 626 g and 23 l/h is considerably above the distribution with a carbon black fraction of 25 %, a high carbon black separation efficiency over 25 % can be estimated. As with the sedimentation analysis, the particle size analysis demonstrates that carbon black particles are present in the sediment over the entire characteristic carbon black particle size range down to very low particle sizes.

Table 3 compares the estimated separation efficiencies of the two materials determined by the particle size analysis and the sedimentation analysis. The estimated graphite separation efficiency of at least 90 % determined by the particle size analysis correspond to the results of the same centrate samples measured by the sedimentation analysis. The carbon black separation efficiency between 10 % and 25 % estimated by the particle size analysis for 626 g and 66 l/h is in the same range of the carbon black separation efficiency of over 20 % measured by the sedimentation analysis for these operation parameters. The carbon black fractions in the sediment determined by the two analytical methods for 626 g and 23 l/h are also in the same range. While the particle size distribution of the sediment sample at 626 g and 23 l/h is considerably above the distribution with a carbon black fraction of 25 %, the sedimentation analysis also yields a higher carbon black fraction in the sediment of significantly above 20 %. Overall, both analytical methods provide matching results for both the centrate and the sediment.

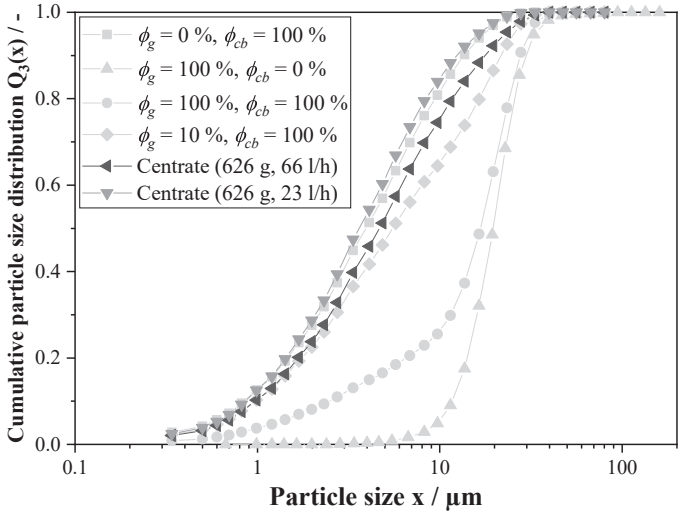

Fig. 14. Cumulative particle size distributions of reference measurements and centrate samples taken at a constant centrifugal acceleration of 626 g and different volume flows from the decanter centrifuge.

4. Conclusions

To evaluate the fractionation of an anode slurry into the active material graphite and the conductive additive carbon black by using a decanter centrifuge, two analytical methods for the determination of graphite and carbon black fractions in centrate and sediment samples were successfully developed and tested. Particle size analysis by a laser diffraction instrument can estimate graphite and carbon black fractions down to 10 % in carbon-black- and graphite-rich slurries. The sedimentation analysis with the developed concentrating method can also be used to determine down to approx. 10 % graphite fraction in a carbon-black-rich slurry. The detectability of carbon black in a graphite-rich slurry by the sedimentation analysis with the LUMiSizer©, is significantly more sensitive with a carbon black fraction of down to 1 % due to the strong light extinction behavior of carbon black.

The application of the analytical methods to centrate and sediment samples taken from the decanter centrifuges at different operation conditions results in high graphite separation of at least 90 % in all cases. The lowest carbon black deposition between 10 % and 20 % was observed for a centrifugal acceleration of 352 g at a volume flow of 66 l/h. Both analytical methods provide similar carbon black and graphite separation efficiencies and can track the typical influences of process parameters on particle separation in the decanter centrifuge, such as increasing particle separation by lowering the volume flow or rising centrifugal acceleration. It should be noted that a selective fractionation of an aqueous anode suspension into graphite and carbon black in the decanter centrifuge is basically possible even at a high solid volume fraction and thus represents a suitable process for the direct recycling of LIB.

To keep the carbon black separation even lower, a dispersion step e. g. by ultrasonic treatment prior to centrifugation is imaginable to avoid heteroagglomerates between graphite and carbon black and to break down carbon black agglomerates to smaller aggregate size. The potential of centrifugation to separate a cathode slurry into carbon black in the centrate and the cathode active material in the sediment, already investigated by Wolf et al. [34], and to separate an anode slurry into carbon black in the centrate and the anode active material in the sediment has now been successfully demonstrated. Therefore, the applicability of the centrifugation process to a real black mass slurry from end-of-life lithium-ion batteries to separate the carbon black, the anode active material, and the cathode active material is also of future interest.

CRediT authorship contribution statement

Tolga Yildiz: Project administration, Conceptualization, Data curation, Methodology, Visualization, Writing – original draft, Validation, Formal analysis, Resources. **Patrick Wiechers**: Conceptualization, Methodology, Investigation, Data curation. **Hermann Nirschl**: Supervision, Writing – review & editing, Funding acquisition. **Marco Gleiß**: Supervision, Writing – review & editing, Funding acquisition.

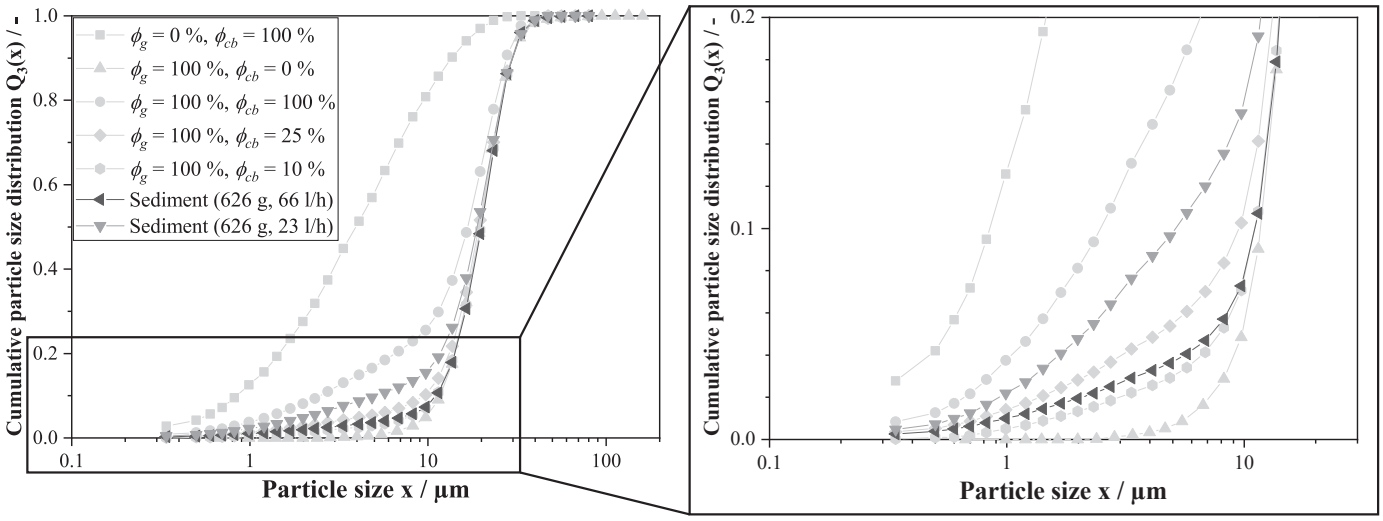

Fig. 15. Cumulative particle size distributions of reference measurements and sediment samples taken at a constant centrifugal acceleration of 626 g and different volume flows from the decanter centrifuge.

Table 3
Separation efficiencies of graphite (η_g) and carbon black (η_{cb}) for different centrifugal accelerations and volume flows estimated by the sedimentation analysis (SA) with the LUMiSizer© and by particle size analysis (PSA) with laser diffraction.

Centrifugal acceleration / g	Volume flow / l/h	η_g (SA) / %	η_g (PSA) / %	η_{cb} (SA) / %	η_{cb} (PSA) / %
352	23	> 90	–	> 20	–
	43	> 90	–	10–20	–
	66	> 90	–	10–20	–
626	23	> 90	> 90	> 20	> 25
	43	> 90	–	> 20	–
	66	> 90	> 90	> 20	10–25

Declaration of Competing Interest

The authors declare that they have no known competing financial interests or personal relationships that could have appeared to influence the work reported in this paper.

Acknowledgements

The project HydroLIBRec on which this publication is based was funded by the German Federal Ministry of Education and Research within the Competence Cluster Recycling & Green Battery (greenBatt) under the grant number 03XP0339C. The authors are responsible for the contents of this publication.

References

[1] C. Capasso, O. Veneri, Experimental analysis on the performance of lithium based batteries for road full electric and hybrid vehicles, Appl. Energy 136 (2014) 921–930, https://doi.org/10.1016/j.apenergy.2014.04.013.
[2] B. Diouf, R. Pode, Potential of lithium-ion batteries in renewable energy, Renew. Energy 76 (2015) 375–380, https://doi.org/10.1016/j.renene.2014.11.058.
[3] J.W. Choi, D. Aurbach, Promise and reality of post-lithium-ion batteries with high energy densities, Nat. Rev. Mater. 1 (4) (2016) 1–16, https://doi.org/10.1038/natrevmats.2016.13.
[4] A. Manthiram, An outlook on lithium ion battery technology, ACS Cent. Sci. 3 (10) (2017) 1063–1069, https://doi.org/10.1021/acscentsci.7b00288.
[5] European Comission Directive 2006/66/EC of The European Parliament and of the Council of 6. September 2006 on batteries and accumulators and waste batteries and accumulators and repealing Directive 91/157/EEC.2006.
[6] X. Zheng, Z. Zhu, X. Lin, Y. Zhang, Y. He, H. Cao, Z. Sun, A mini-review on metal recycling from spent lithium ion batteries, Engineering 4 (3) (2018) 361–370, https://doi.org/10.1016/j.eng.2018.05.018.
[7] E. Mossali, N. Picone, L. Gentilini, O. Rodrìguez, J.M. Pérez, M. Colledani, Lithium-ion batteries towards circular economy: a literature review of opportunities and issues of recycling treatments, J. Environ. Manag. 264 (2020), 110500, https://doi.org/10.1016/j.jenvman.2020.110500.
[8] Z.J. Baum, R.E. Bird, X. Yu, J. Ma, Lithium-ion battery recycling - overview of techniques and, trends (2022), https://doi.org/10.1021/acsenergylett.1c02602.
[9] Council of the European Union Proposal for a regulation of the european parliament and of the council concerning batteries and waste batteries, repealing directive 2006/66/ec and amending regulation (eu) no 2019/1020.2023.
[10] P. Meister, H. Jia, J. Li, R. Kloepsch, M. Winter, T. Placke, Best practice: performance and cost evaluation of lithium ion battery active materials with special emphasis on energy efficiency, Chem. Mater. 28 (20) (2016) 7203–7217, https://doi.org/10.1021/acs.chemmater.6b02895.
[11] H. Zhang, Y. Yang, D. Ren, L. Wang, X. He, Graphite as anode materials: fundamental mechanism, recent progress and advances, Energy Storage Mater. 36 (2021) 147–170, https://doi.org/10.1016/j.ensm.2020.12.027.
[12] S. Natarajan, M.L. Divya, V. Aravindan, Should we recycle the graphite from spent lithium-ion batteries? the untold story of graphite with the importance of recycling, J. Energy Chem. 71 (2022) 351–369, https://doi.org/10.1016/j.jechem.2022.04.012.
[13] O. Velázquez-Martínez, J. Valio, A. Santasalo-Aarnio, M. Reuter, R. Serna-Guerrero, A critical review of lithium-ion battery recycling processes from a circular economy perspective, Batteries 5 (4) (2019) 68, https://doi.org/10.3390/batteries5040068.
[14] M. Assefi, S. Maroufi, Y. Yamauchi, V. Sahajwalla, Pyrometallurgical recycling of li-ion, ni–cd and ni–mh batteries: a minireview, Curr. Opin. Green. Sustain. Chem. 24 (2020) 26–31, https://doi.org/10.1016/j.cogsc.2020.01.005.
[15] B. Makuza, Q. Tian, X. Guo, K. Chattopadhyay, D. Yu, Pyrometallurgical options for recycling spent lithium-ion batteries: a comprehensive review, J. Power Sources 491 (2021), 229622, https://doi.org/10.1016/j.jpowsour.2021.229622.
[16] Y. Yao, M. Zhu, Z. Zhao, B. Tong, Y. Fan, Z. Hua, Hydrometallurgical processes for recycling spent lithium-ion batteries: a critical review, ACS Sustain. Chem. Eng. 6 (11) (2018) 13611–13627, https://doi.org/10.1021/acssuschemeng.8b03545.
[17] J.C.-Y. Jung, P.-C. Sui, J. Zhang, A review of recycling spent lithium-ion battery cathode materials using hydrometallurgical treatments, J. Energy Storage 35 (2021), 102217, https://doi.org/10.1016/j.est.2020.102217.
[18] L. Gaines, K. Richa, J. Spangenberger, Key issues for li-ion battery recycling, MRS Energy Sustain. 5 (2018), E14, https://doi.org/10.1557/mre.2018.13.
[19] M. Chen, X. Ma, B. Chen, R. Arsenault, P. Karlson, N. Simon, Y. Wang, Recycling end-of-life electric vehicle lithium-ion batteries, Joule 3 (11) (2019) 2622–2646, https://doi.org/10.1016/j.joule.2019.09.014.
[20] L. Gaines, The future of automotive lithium-ion battery recycling: charting a sustainable course, Sustain. Mater. Technol. 1 (2014) 2–7, https://doi.org/10.1016/j.susmat.2014.10.001.
[21] G. Harper, R. Sommerville, E. Kendrick, L. Driscoll, P. Slater, R. Stolkin, A. Walton, P. Christensen, O. Heidrich, S. Lambert, et al., Recycling lithium-ion batteries from electric vehicles, nature 575 (7781) (2019) 75–86, https://doi.org/10.1038/s41586-019-1682-5.
[22] J. Wu, M. Zheng, T. Liu, Y. Wang, Y. Liu, J. Nai, L. Zhang, S. Zhang, X. Tao, Direct recovery: a sustainable recycling technology for spent lithium-ion battery, Energy Storage Mater. 54 (2023) 120–134, https://doi.org/10.1016/j.ensm.2022.09.029.
[23] Y. Kim, M. Matsuda, A. Shibayama, T. Fujita, Recovery of LiCoO2 from wasted lithium ion batteries by using mineral processing technology, Resour. Process. 51 (1) (2004) 3–7, https://doi.org/10.4144/rpsj.51.3.
[24] R. Zhan, Z. Oldenburg, L. Pan, Recovery of active cathode materials from lithium-ion batteries using froth flotation, Sustain. Mater. Technol. 17 (2018), e00062, https://doi.org/10.1016/j.susmat.2018.e00062.

[25] A. Vanderbruggen, A. Salces, A. Ferreira, M. Rudolph, R. Serna-Guerrero, Improving separation efficiency in end-of-life lithium-ion batteries flotation using attrition pre-treatment, Minerals 12 (1) (2022) 72, https://doi.org/10.3390/min12010072.

[26] H. Anlauf, Recent developments in centrifuge technology, Sep. Purif. Technol. 58 (2) (2007) 242–246, https://doi.org/10.1016/j.seppur.2007.05.012.

[27] W.W.-F. Leung, 1 - introduction, in: W.W.-F. Leung (Ed.), Centrifugal Separations in Biotechnology, Second edition, Butterworth-Heinemann, 2020, pp. 1–25, https://doi.org/10.1016/B978-0-08-102634-2.00001-5.

[28] G.G. Stokes, et al., On the effect of the internal friction of fluids on the motion of pendulums.2010.

[29] K.D. Kepler, F. Tsang, R. Vermeulen, P. Hailey, Process for recycling electrode materials from lithium-ion batteries, US Patent 9,614,261 (2017).

[30] H. Al-Shammari, S. Farhad, Regeneration of cathode mixture active materials obtained from recycled lithium ion batteries, Tech. rep., SAE Technical Paper (2020), https://doi.org/10.4271/2020–01-0864.

[31] H. Al-Shammari, S. Farhad, Heavy liquids for rapid separation of cathode and anode active materials from recycled lithium-ion batteries, Resour., Conserv. Recycl. 174 (2021), 105749, https://doi.org/10.1016/j.resconrec.2021.105749.

[32] Y. Zhang, Y. He, T. Zhang, X. Zhu, Y. Feng, G. Zhang, X. Bai, Application of falcon centrifuge in the recycling of electrode materials from spent lithium ion batteries, J. Clean. Prod. 202 (2018) 736–747, https://doi.org/10.1016/j.jclepro.2018.08.133.

[33] R. Zhan, L. Pan, A cycling-insensitive recycling method for producing lithium transition metal oxide from li-ion batteries using centrifugal gravity separation, Sustain. Mater. Technol. 32 (2022), e00399, https://doi.org/10.1016/j.susmat.2022.e00399.

[34] A. Wolf, A. Flegler, J. Prieschl, T. Stuebinger, W. Witt, F. Seiser, T. Vinnay, T. Sinn, M. Gleiß, H. Nirschl, et al., Centrifugation based separation of lithium iron phosphate (lfp) and carbon black for lithium-ion battery recycling, Chem. Eng. Process. -Process. Intensif. 160 (2021), 108310, https://doi.org/10.1016/j.cep.2021.108310.

[35] A. Records, K. Sutherland, Chapter 1 - introduction, in: A. Records, K. Sutherland (Eds.), Decanter Centrifuge Handbook, Elsevier, Amsterdam, 2001, pp. 1–14, https://doi.org/10.1016/B978-185617369-8/50001-0.

[36] E. Tarleton, R. Wakeman, 1 - solid/liquid separation equipment, in: E. Tarleton, R. Wakeman (Eds.), Solid/Liquid Separation, Butterworth-Heinemann, Oxford, 2007, pp. 1–77, https://doi.org/10.1016/B978-185617421-3/50001-8.

[37] J.-T. Li, Z.-Y. Wu, Y.-Q. Lu, Y. Zhou, Q.-S. Huang, L. Huang, S.-G. Sun, Water soluble binder, an electrochemical performance booster for electrode materials with high energy density, Adv. Energy Mater. 7 (24) (2017), 1701185, https://doi.org/10.1002/aenm.201701185.

[38] J. Li, Y. Lu, T. Yang, D. Ge, D.L. Wood, Z. Li, Water-based electrode manufacturing and direct recycling of lithium-ion battery electrodes—a green and sustainable manufacturing system, IScience 23 (5) (2020), https://doi.org/10.1016/j.isci.2020.101081.

[39] G. Bickert, Sedimentation feinster suspendierter partikeln im zentrifugalfeld, Ph.D. thesis, University Fridericiana Karlsruhe (1997).

[40] M. Beiser, Sedimentation submikroner partikel in abhängigkeit physikalisch-chemischer einflüsse und ihr separationsverhalten in dekantierzentrifugen, Ph.D. thesis, Dissertation. Universität Karlsruhe (TH)(2006).

[41] D. Lerche, Dispersion stability and particle characterization by sedimentation kinetics in a centrifugal field, J. Dispers. Sci. Technol. 23 (5) (2002) 699–709, https://doi.org/10.1081/DIS-120015373.